Time-domain spectrum of dielectric relaxation in relaxor ferroelectrics: Monte Carlo simulation

2006 J. Phys.: Condens. Matter 18 8973

(http://iopscience.iop.org/0953-8984/18/39/026)

INSTITUTE OF PHYSICS PUBLISHING JOURNAL OF PHYSICS: CONDENSED MATTER

J. Phys.: Condens. Matter **18** (2006) 8973–8985 doi:10.1088/0953-8984/18/39/026

Time-domain spectrum of dielectric relaxation in relaxor ferroelectrics: Monte Carlo simulation

J-M Liu[1,2,3,4], **S Dong**[2], **H L W Chan**[1,2] **and C L Choy**[1,2]

[1] Department of Applied Physics, Hong Kong Polytechnic University, Hong Kong, People's Republic of China
[2] Nanjing National Laboratory of Microstructures, Nanjing University, Nanjing 210093, People's Republic of China
[3] International Center for Materials Physics, Chinese Academy of Sciences, Shenyang, People's Republic of China

E-mail: liujm@nju.edu.cn

Received 10 February 2006, in final form 13 July 2006
Published 15 September 2006
Online at stacks.iop.org/JPhysCM/18/8973

Abstract

We perform Monte Carlo simulation on the dielectric relaxation behaviour of a model relaxor ferroelectric, based on the Ginzburg–Landau theory of ferroelectrics with dipole-defect induced random field. The coexistence of ferroelectric nanoclusters and paraelectric matrix is demonstrated. It is found that the time-domain spectrum for dielectric relaxation below the ferroelectric transition point exhibits a multi-peaked pattern rather than the diffusive single-peaked pattern, indicating the existence of multi-characteristic times for the dielectric relaxation. The extended multi-peaked time-domain spectrum is responsible for the diffusive ferroelectric transitions and frequency dispersion of the dielectric relaxation, usually observed for relaxor ferroelectrics.

1. Introduction

Relaxor ferroelectrics (RFEs) like $Pb(Mg_{1/3}Nb_{2/3})O_3$ have been receiving continuous attentions because of their unusual ferroelectric transitions and excellent electromechanical coupling performances. These unusual behaviours are commonly ascribed to the abnormal domain structure of RFEs that is different from that of a normal ferroelectric (FE): the coexistence of FE nanoclusters embedded in paraelectric (PE) matrix below the FE transition point T_c if definable [1–4]. Consequently, the dielectric relaxation as a function of temperature T shows diffusive phase transitions and strong frequency dispersion [5]. The FE behaviours of RFEs are featured with the frequency-dependent hysteresis in the PE state and weak FE hysteresis below T_c. Therefore, a comprehensive understanding of the two-phase coexistence structure of RFEs at the nanoscale becomes particularly attractive.

[4] Author to whom any correspondence should be addressed.

First of all, because of the two-phase coexistence characters, the dynamic response of RFEs to external fluctuations (e.g. ac electric field) can be very different from that of normal FEs, where the long-range FE ordering does not allow sufficient relaxation of local dipoles alone due to the dipole interaction. However, the nanosized FE clusters in RFEs may respond to external fluctuations either by local dipole reorientation or through a spatial shift from their equilibrium positions, or both [6]. In addition, to our common understanding, it is believed that the size of these clusters exhibits a broad distribution, leading to significant inhomogeneity in terms of local dipole relaxation and temperature-dependent FE transitions [7]. If each dipole is treated as a relaxator and no interaction between these relaxators is considered, an RFE usually offers a very broad monotonic or single-peaked distribution of relaxation time, thus resulting in diffusive phase transitions and remarkable frequency dependence of the dielectric relaxation. However, one has reason to argue that the dipoles inside one FE nanocluster are not independent of one another, and also the inter-cluster interaction could be significant.

Secondly, the dipole glass-like behaviours of RFEs have been extensively studied [5, 8]. The broad distribution of dipole relaxation time is retained at temperature T around T_c. When T decreases, the FE clusters may grow and coalesce, and finally be frozen at temperature $T_f \ll T_c$, leading to a frozen polar glass-like state to which the well-known Vogel–Fulcher relationship may apply [7]. This relationship is accepted to be one of the criteria to justify RFEs from experimental aspects [9, 10]. The Vogel–Fulcher mode above T_f describes the thermally activated process in a dipole cluster glass system, which can be understood in the framework of thermal dipole flip (dipole reorientation and spatial shift of FE clusters). For $T < T_f$, it is argued that the thermal dipole flip alone no longer makes sense; at least it may not be the dominant mechanism for RFE behaviours [10].

The above discussion advises us that the time-domain distribution of dielectric relaxation is a key to our understanding of RFEs. Given the external field fluctuations, the time-domain distribution of dielectric relaxation, $G(\log\tau, T)$, where τ is the relaxation time, determines uniquely the dielectric relaxation behaviours [11], enabling us to evaluate the dielectric response of RFEs over the whole time (or frequency) domain and providing us with helpful information on the dipole configuration. As a consequence, the FE and electromechanical performance can be predicted in a more reliable manner.

Current theories on RFEs assume that an RFE is composed of an ensemble of relaxators, which are independent of each other [11]. The distribution, $G(\log\tau, T)$, against τ must be either monotonic or single-peaked over the whole time domain [7]. Nevertheless, for RFEs, if the dipole glass-like behaviour is of general significance and the picture of the two-phase coexistence in the nanoscale applies, one may argue that the interactions between these FE cluster-pairs at $T < T_c$ are no longer negligible. The distribution $G(\log\tau, T)$ may be single-peaked at $T > T_c$, because the dipoles and clusters are well separated and their interaction is negligible. However, the distribution at $T < T_c$ may no longer be monotonic or single-peaked (diffusive) because of the FE cluster essence and significant inter-cluster interactions. One has reason to argue that $G(\log\tau, T)$ at $T < T_c$ is double-peaked or multi-peaked, depending on the relaxation of interacting FE clusters and the PE matrix phase surrounding these clusters. Although the single-peaked feature of $G(\log\tau, T)$ was indicated experimentally [7, 12, 13], the evidence is indirect because the data are derived from reconstructed dielectric response functions. This means that the outcome may not be unique. In other words, there has never been direct evidence on the pattern of $G(\log\tau, T)$ reported so far, although the measured dielectric dispersion is always diffusive and single-peaked. Nevertheless, some recent experiment on typical RFE 90PMN-10PT systems by Röhmer's group [14], based on the nonresonant dielectric hole-burning technique, detected successfully the time distribution of dynamic relaxation in response to external pump field, indicating a significant effect of some kinds of

domain pinning barriers on the dynamic relaxation. It is believed from this experiment that the interaction between the nanosized domains as subensembles is indeed significant.

In this paper, we will investigate the time-domain distribution $G(\log\tau, T)$ for a model RFE. Our major interest will be in those theoretical models from which $G(\log\tau, T)$ can be directly evaluated. For RFEs, the extensively studied models include the dipole-glass model [5], the superparaelectric model [8], and the compositional inhomogeneity scheme [15], among others, which describe the dipole configuration of RFEs in a framework of standard dipole interactions coupled with internal random field. Unfortunately, up to now a generalized model, which can reasonably interpret all features of RFEs, seems unavailable to us. Here, we employ the Ginzburg–Landau model on ferroelectrics that was proposed recently [16] to describe the relaxation dynamics of RFEs, in which the thermally activated dipole flip is assumed to be the unique mechanism for dielectric relaxation. This assumption implies that the present model may not be applicable to cases of $T < T_f$ where the dipole clusters are frozen. In this model, a special type of dipole defect is considered, which is responsible for the relaxor-like behaviours in some doped ferroelectrics [17]. These defects can be either impurity atoms distributed randomly in the lattice or off-centre dopant ions which generate the so-called internal random fields or random bonds, or even a frustration of the long-range ordering state. This model can be identified by quite a lot of experimental findings where a normal FE evolves into an RFE by doping, such as the well known Zr(Hf)-doped $BaTiO_3$ and La(Pr)-doped $Pb(Zr, Ti)O_3$. The essential roles of the dipole defects in modulating a normal FE into an RFE were investigated earlier and no details will be given here [18]. We perform Monte Carlo (MC) simulation on the lattice configuration of electric dipoles and dielectric relaxation behaviours in this defective FE lattice as a model RFE, from which the time-domain distribution of the relaxation can be directly evaluated. An interesting finding is that the time-domain distribution of the dielectric relaxation is indeed multi-peaked instead of single-peaked or diffusive single-peaked. We leave the dynamic details of the dielectric relaxation, such as frequency dispersion and Vogel–Fulcher relationship, to be reported elsewhere [19].

2. Model and simulation

The MC simulation is performed on a two-dimensional (2D) $L \times L$ lattice with periodic boundary conditions, where the PE and FE phases take the square and rectangular configurations, respectively. For a reliable simulation, a 3D lattice should be employed. However, the computational requirement is extremely big and because we do not focus much on the critical phenomena associated with the FE phase transitions, all of our simulations will be performed on a 2D lattice. We once employed a $16 \times 16 \times 16$ cubic lattice for a pre-simulation and did not find significant difference of the simulated results (e.g. dielectric relaxation) from those we obtained for a 2D lattice of $L \sim 64$. The simulation starts from the Ginzburg–Landau model and a detailed introduction to this model was given earlier [20]. In short, for each lattice site, a dipole vector $\boldsymbol{P}$ is assigned with its moment and orientation defined by the energy minimization. We define $\boldsymbol{P} = (P_x(\boldsymbol{r}), P_y(\boldsymbol{r}))$ where P_x and P_y are the two components along x- and y-axis, respectively, and consider the contributions from the Landau double-well potential, the long-range dipole–dipole interaction and gradient energy associated with domain walls. The long-range elastic energy will not be taken into account [18]. The Landau double-well potential f_L can be written as

$$f_L(P_i) = A_1(P_x^2 + P_y^2) + A_{11}(P_x^4 + P_y^4) + A_{12}P_x^2P_y^2 + A_{111}(P_x^6 + P_y^6) \tag{1}$$

where subscript i refers to lattice site i, and A_1, A_{11}, A_{12} and A_{111} are the energy coefficients, respectively. For a normal FE, a first-order FE transition will occur if $A_1 < 0$. In the present

model, the dipole vector is assumed to take one of the four orientations: [1, 0], [−1, 0], [0, 1] and [0, −1]. The gradient energy for the polarization field is written as below:

$$f_{\mathrm{G}}(P_{i,j}) = \tfrac{1}{2}G_{11}(P_{x,x}^2 + P_{y,y}^2) + G_{12}P_{x,x}P_{y,y} + \tfrac{1}{2}G_{44}(P_{x,y} + P_{y,x})^2 + \tfrac{1}{2}G'_{44}(P_{x,y} - P_{y,x})^2 \tag{2}$$

where $P_{i,j} = \partial P_i/\partial x_j$. Parameters G_{11}, G_{12}, G_{44} and G'_{44} are all positive, indicating that any dipole fluctuation in either moment or orientation is not favoured. This gradient term prefers long-range FE ordering. Furthermore, the dipole–dipole interaction is long-ranged and it should be considered for an inhomogeneous system. In SI units, the energy for site i can be written as

$$f_{\mathrm{dip}}(P_i) = \frac{1}{8\pi\varepsilon_0\chi}\sum_{\langle j\rangle}\left[\frac{P(r_i)\cdot P(r_j)}{|r_i - r_j|^3} - \frac{3\left[P(r_i)\cdot(r_i - r_j)\right]\left[P(r_j)\cdot(r_i - r_j)\right]}{|r_i - r_j|^5}\right] \tag{3}$$

where $\langle j\rangle$ represents a summation over all sites within a separation radius R centred at site i, parameters r_i, r_j, $P(r_i)$ and $P(r_j)$ here should be vectors, and r_i and r_j are the coordinates of sites i and j, respectively. In a strict sense, R should be infinite but an effective cut-off at $R = 8$ is taken in our simulation [21]. Finally, the electrostatic energy induced by external electric field is

$$f_{\mathrm{E}}(P_i) = -P_i \cdot E \tag{4}$$

where E is external electric field, which takes the [1, 0] orientation in our simulation. The Hamiltonian for the system is

$$H = \sum_{\langle i\rangle} f_{\mathrm{L}} + f_{\mathrm{G}} + f_{\mathrm{dip}} + f_{\mathrm{E}} \tag{5}$$

where $\langle i\rangle$ refers to the summation over the whole lattice.

The dipole defects and thus the internal random field are introduced into the lattice by imposing random magnitude fluctuations to parameter A_1, while the others remain unchanged. One may refer to earlier reports on detailed discussion [16, 18]. We have

$$\begin{aligned} &A_1(r_i) = A_{10} + b_m \cdot c \\ &A_{10} = \alpha(T - T^0), \qquad \alpha > 0 \end{aligned} \tag{6}$$

where $\alpha > 0$ is a materials constant, A_{10} is the coefficient A_1 in equation (1), T^0 is the critical temperature for a normal FE crystal, c takes 0 or 1 to represent a perfect site or a defective site, and b_m is the coefficient characterizing the influence of defects on T^0 and can be written as $b_m = -\alpha\frac{\mathrm{d}T^0(C_0)}{\mathrm{d}C_0}$, where C_0 is the average concentration of defects in the lattice. We take the case of $T = T^0$ as an illustration without losing generality. For a lattice site i, $A_1(r_i) > 0$ if $b_m > 0$, implying suppressed ferroelectricity, and $A_1(r_i) < 0$ if $b_m < 0$, enhanced ferroelectricity. We define the second defect concentration variable $C_p \in [0, 1]$, which means $C_0 \cdot C_p \cdot L^2$ defect lattice sites with $b_m > 0$ and the remaining $C_0 \cdot (1 - C_p) \cdot L^2$ sites with $b_m < 0$. The value of b_m for a site is randomly taken from range $[0.5, 1.0]b_M$ for $b_m > 0$ and $[-0.5, -1.0]b_M$ for $b_m < 0$, with a given $b_M > 0$. We shall simulate the dielectric relaxation in such an RFE system.

The dielectric relaxation of the RFE is characterized by the dynamic dielectric susceptibility $\chi = \chi' + \mathrm{i}\chi''$, defined as [16, 17]

$$\begin{aligned} \chi' &= \frac{C}{NT}\left\langle\sum_i^N \frac{1}{1 + (\omega\cdot\tau_i/\omega_0)^2}\right\rangle \\ \chi'' &= \frac{C}{NT}\left\langle\sum_i^N \frac{\omega\cdot\tau_i/\omega_0}{1 + (\omega\cdot\tau_i/\omega_0)^2}\right\rangle \end{aligned} \tag{7}$$

where χ' and χ'' are the real and imaginary parts of χ, $\langle\ \rangle$ represents the configuration

averaging, the summation is performed over the whole lattice, ω_0 is the polariton frequency which is a material constant, $N = L^2$ and C is a temperature-independent constant. In our simulation here, $\omega_0 = 1$ is assumed for simplification. Here, time τ_i at site i depends on both the local Landau potential and dipole flip among those candidate states at site i, which can be written as

$$\tau_i = \tau_0 \cdot \tau' = \tau_{00} \exp(-f_{\mathrm{L}}/kT) \cdot \tau' \tag{8}$$

where τ_0 is the characteristic flip time for a non-interacting system, which is actually determined by the energy barrier referring to the Landau free energy f_{L} at site i, $\tau_{00} = 1.0$ is the pre-exponential factor which scales the characteristic time for lattice vibration, and τ' is the averaged inverse number of flips for the dipole at site i *per Monte Carlo step (mcs)*. The detailed procedure of the simulation was reported earlier [18]. In the simulation, $b_M = 5.0$ and $C_0 = 0.5$ are fixed, and C_p is treated as a variable. The other lattice parameters used in the simulation were chosen and the dimensionless normalization of them was done following the works of Hu *et al* [22] on the dynamics of domain switching in the $BaTiO_3$ system. In addition, the external electric field $E = E_m \cdot \sin(2\pi\omega \cdot t)$, where E_m is the ac signal amplitude and t is time. We take $T^0 = 4.0$ in our simulation.

3. Results of simulation and discussion

Figure 1 presents the snapshots of simulated dipole configurations for a normal FE ($C_0 = 0$, left column) and RFE ($C_0 = 0.5$, $C_p = 0.5$, right column) at $T = 4.0$, 2.5 and 1.5, respectively. It is shown that at $T = T^0 = 4.0$, the normal FE system shows a homogeneous PE phase over the whole lattice (figure 1(a)). With defects induced into the lattice, although the spatial distribution of the defects is random, local FE clusters as indicated by the open circles become evident at $T \sim T^0$, above the FE transition point ($T_{\mathrm{c}} < T^0$), as shown in figure 1(b), exhibiting typical RFE features. These features can be more clearly identified at $T = 2.5$, as shown in figure 1(d). While the normal FE lattice exhibits typical multi-domained dipole configuration shown in figure 1(c), the coexistence of FE nanoclusters and a PE matrix is identified. With further decreasing of T down to 0.5, as shown in figures 1(e) and (f), both the FE and RFE systems exhibit a multi-domained lattice and not much PE phase in the RFE lattice can be observed. These features were reported in detail in our previous works [18].

To look at the dielectric relaxation behaviours, we present the dielectric susceptibility (real and imaginary parts, χ' and χ'') as a function of T in the insets of figure 2 for different defect concentrations C_0 ($C_p = 0.5$) at $E_m = 15.0$ and $\omega = 0.5$ mcs^{-1}. For a normal FE ($C_0 = 0$), a sharp FE transition is observed from the χ'–T relationship although χ' at the transition point does not reach infinity due to the limited lattice size for simulation. For $C_0 = 0.5$ and 1.0, one observes clearly a broadening of the transition peaks in both χ'–T and χ''–T curves, a common feature for RFEs. This broadening becomes very remarkable at $C_0 = 1.0$, indicating significant diffusive behaviour of the FE transitions. By replotting the data in χ'–$\log T$ and χ''–$\log T$ coordinate format, one sees the transition broadening more clearly. In particular, one may speculate that the χ'–$\log T$ curve at $C_0 = 0.5$ is probably an overlap of a series of FE transitions occurring consecutively over a temperature range. This is a strong hint for a multi-peaked distribution of the dielectric relaxation in RFEs.

To confirm this speculation, we evaluate the time-domain distribution of the dielectric relaxation, i.e. $G(\log\tau, T)$, satisfying [7, 11]

$$\begin{aligned} &\int_0^\infty G(\log\tau, T) \cdot \mathrm{d}(\log\tau) = 1 \\ &\chi'(\omega, T) = \chi'_{\mathrm{s}} \int_0^T G(\log\tau, T) \cdot \mathrm{d}(\log\tau) \end{aligned} \tag{9}$$

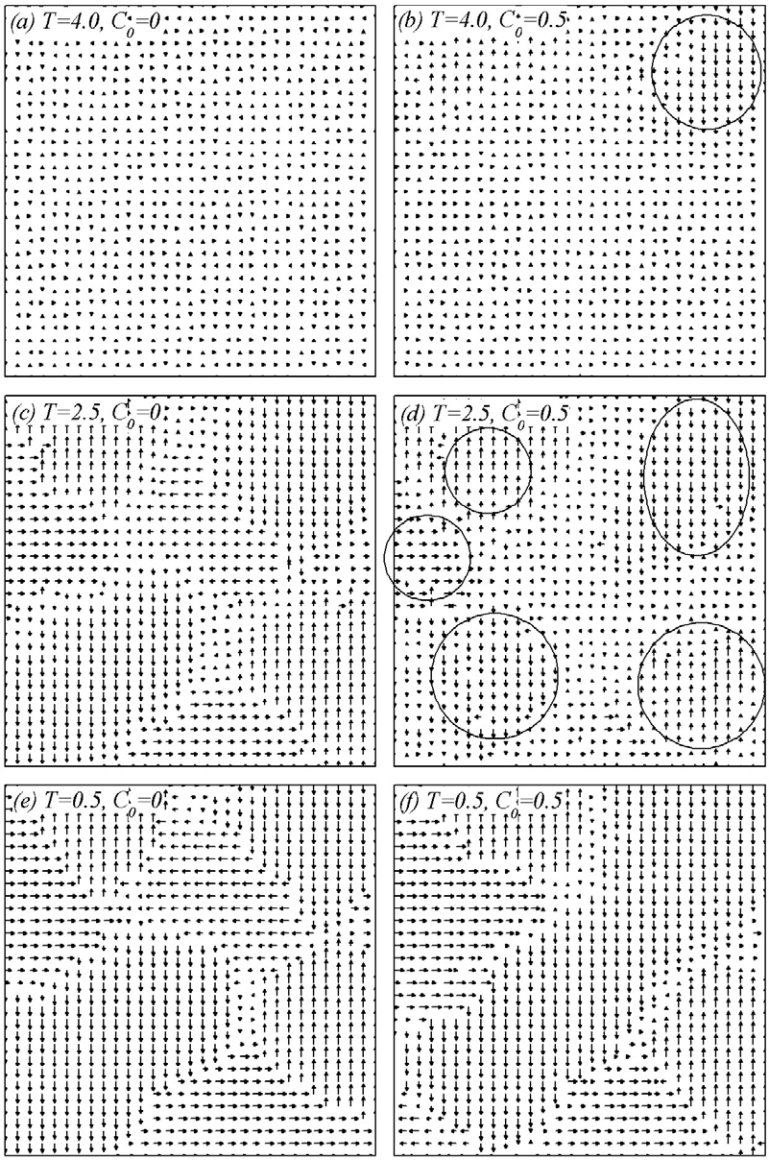

Figure 1. Snapshot dipole configurations for a normal FE lattice (left column) and RFE lattice (right column, $C_0 = 0.5, C_p = 0.5$) at several temperatures as indicated. $T^0 = 4.0$. The open circles enclose the FE nanoclusters.

where χ_s' is the static susceptibility. The evaluated $G(\log\tau, T)$ at several temperatures for a normal FE ($C_0 = 0$), an RFE with $C_0 = 0.5$ and $C_p = 0.0$ (referred to as RFE-I), and an RFE with $C_0 = 0.5$ and $C_p = 1.0$ (referred to as RFE-II), is presented in figures 3(a)–(e), respectively. Here, $E_m = 15$ and $\omega = 0.5$ mcs^{-1}.

From figure 3, one observes that for a normal FE, the distribution $G(\log\tau, T)$ at each temperature is single-peaked. At the PE state, the peak profile is very narrow. With T decreasing into the FE state, the time-domain distribution becomes significantly broadened in the absolute timescale, and the peak position shifts considerably towards the long-time domain.

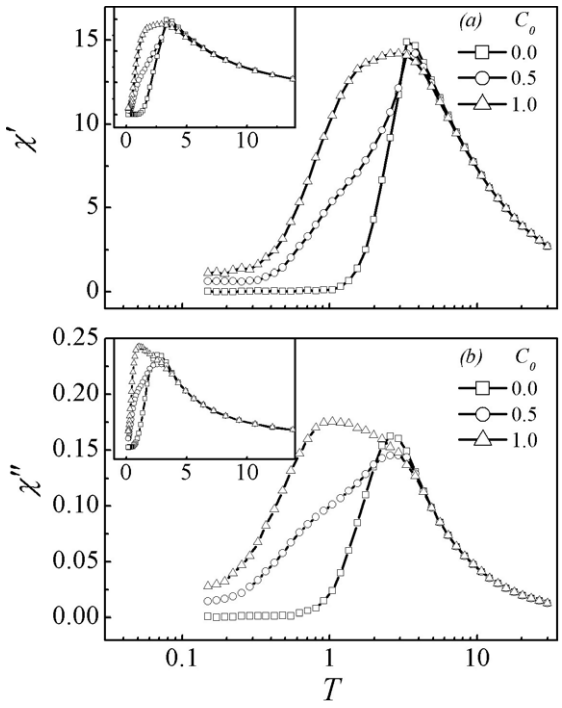

Figure 2. Simulated dielectric susceptibility (real and imaginary parts) as a function of T for various defect concentrations C_0: (a) χ'–log(T) curves and (b) χ''–log(T) curves. The insets show the corresponding χ'–T and χ''–T curves. $C_p = 0.5$, $E_m = 15.0$ and $\omega = 0.5$ mcs^{-1}.

These features are typical for a normal FE where the dipole relaxation is believed to occur rapidly in a cooperative manner due to the long-range dipole ordering. However, the evaluated distribution for RFEs shows very different behaviours. At $T = 6.0$ in the PE state, $G(\log\tau, T)$ is single-peaked, but broader than that of the normal FE. We call this a diffusive single-peaked distribution. The peak position shifts rightward for RFE-I and leftward for RFE-II, with respect to the peak location of the normal FE ($C_0 = 0$). This is understandable because $C_p = 0.0$ and $C_p = 1.0$ correspond respectively to the cases where the dipole defects suppress and enhance the ferroelectricity of the lattice, leading to relatively faster and slower dielectric relaxations, respectively. At $T = 4.0$, close to the normal FE transition point, RFE-I still retains a narrow and single-peaked $G(\log\tau, T)$, but $G(\log\tau, T)$ for RFE-II shows a long tail towards the long-time domain. When T decreases down to 2.0, deep into the two-phase coexistence region for both RFE-I and RFE-II, their $G(\log\tau, T)$ exhibits a double-peaked pattern with one peak locating at the similar position as that of the normal FE (peak-I). The other peak (peak-II) appears in the short-time domain for RFE-I and long-time domain for RFE-II, respectively. When the two peaks become further broadened and separated from each other with decreasing T, peak-II eventually smears out and covers a very broad time domain while peak-I remains relatively sharp at extremely low $T = 0.5$. This is a clear indication that the FE nanoclusters are thermally frozen below this temperature.

The above simulations allow us to argue that the time-domain distribution of dielectric relaxation for RFEs in the two-phase coexistence state does not exhibit a diffusive single-peaked pattern, but offers a multi-peaked pattern. The underlying physics is apparently ascribed to the multi-phase coexistence domain structure. Take the two-phase coexistence where the

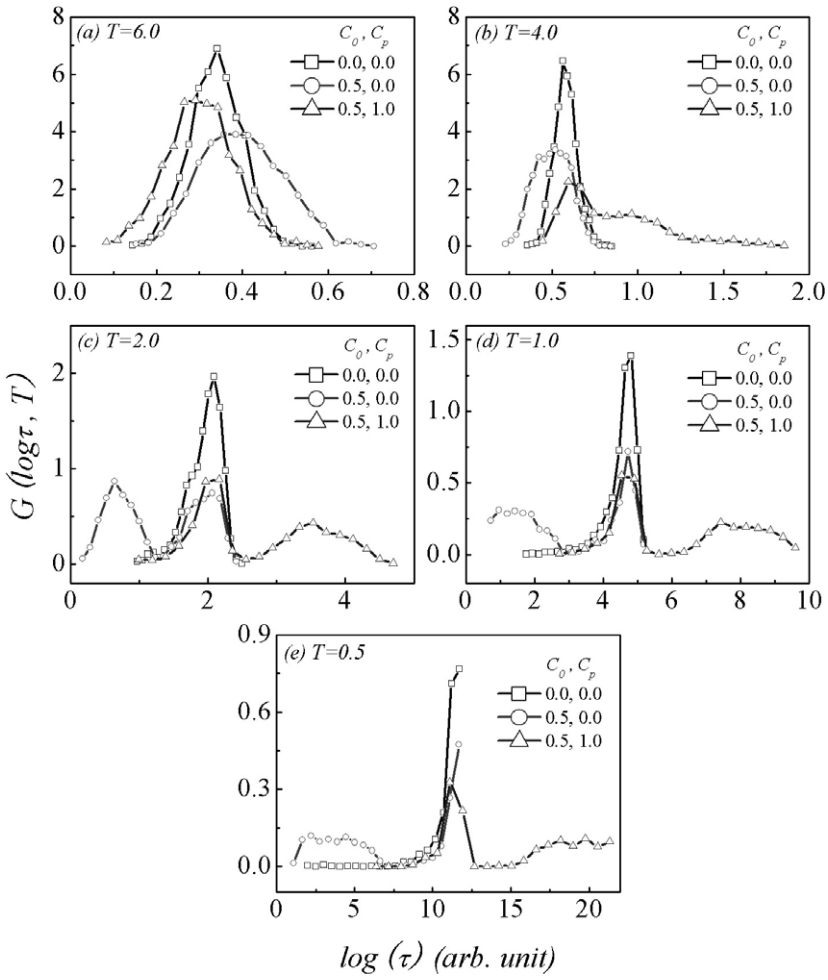

Figure 3. Simulated time-domain distribution $G(\log\tau, T)$ at different T for lattices of various defect concentration C_0 and C_p. $E_m = 15.0$ and $\omega = 0.5$ mcs^{-1}.

FE nanoclusters are similar in size as an example. In a rough sense, the two phases have their own time distributions and characteristic times (peaked times) of dielectric relaxation, respectively. With different types of defects and sizes of FE nanoclusters, the evaluated distribution represents a superposition of the two monotonic or single-peaked distributions. If the peaks of the two distributions are well separated in the time domain, a double-peaked pattern becomes inevitable. Surely, if the random field intensity (b_m) due to the defect doping is not strong enough, these peaks are not widely separated from each other, and a simple superposition of them may give a broad (diffusive) single-peaked distribution, as well believed so far.

In addition to the double-peaked distribution, a multi-peaked distribution is also possible, depending on the doping effect of RFEs. For a two-component doped RFE where one dopant leads to ferroelectric weakening and the other to ferroelectric enhancement, we may take $C_p = 0.5$ to perform a simulation under the same conditions as those shown in figure 3. The simulated time distribution at different T is plotted in figures 4(a)–(c) for a normal FE, and two RFEs with $C_0 = 0.5$ and 1.0, respectively. Again, for the normal FE, the pattern of $G(\log\tau, T)$

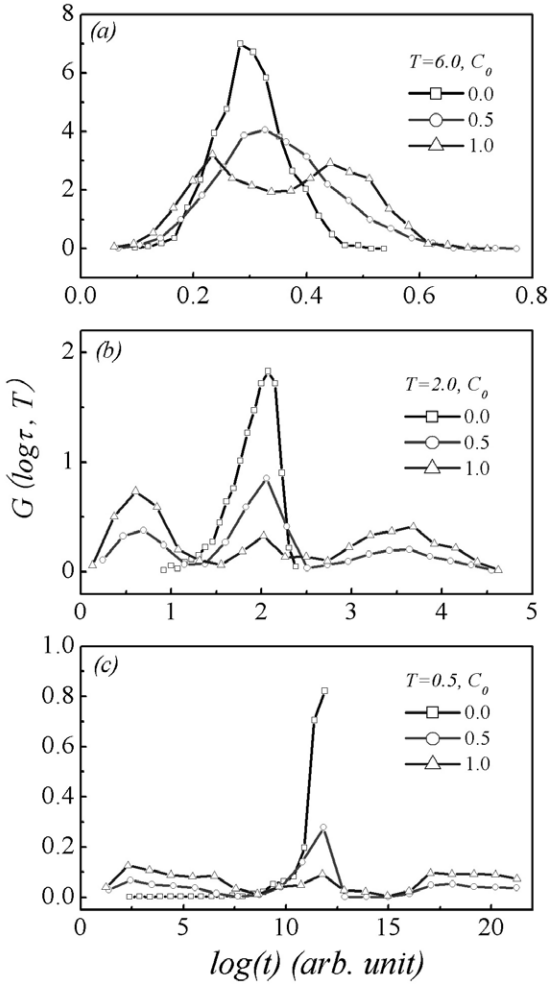

Figure 4. Simulated time-domain distribution $G(\log\tau, T)$ at different T for lattices of various defect concentration C_0. $C_p = 0.5$. $E_m = 15.0$ and $\omega = 0.5$ mcs^{-1}.

is narrow and single-peaked. In comparison to this, $G(\log\tau, T)$ for the RFE with $C_0 = 0.5$ is already broader at $T = 6.0 > T^0$, and then becomes triple-peaked in shape at $T = 2.0$ and 0.5, with the middle peak locating at the similar position as that for the normal FE. This effect can be explained by the fact that $C_0 = 0.5$, i.e. only 50% of the lattice sites are doped with defects and the others remain unaffected. For the RFE with $C_0 = 1.0$, all lattice sites are doped with defects; half of them suppress the ferroelectricity and the remaining half enhance it. The triple-peaked pattern of $G(\log\tau, T)$ rather than a double-peaked shape is expected, even at $T = 6.0 > T^0$. What should be mentioned here is that at extremely low T the distribution covers a very extended time domain, so that the delicate structure of the distribution becomes hardly identified, as shown in figure 4(c) for $C_0 = 1.0$. Furthermore, if the FE nanoclusters are quite different from one another, and/or for a multi-component RFE, a multi-peaked pattern of the time-domain distribution becomes evident.

However, most of the RFEs discovered experimentally by chemical doping may correspond to $C_p = 0$, i.e. RFE-I, and no RFE-II type material has been reported so

far. In fact, Zr(Hf)-doped $BaTiO_3$ and La(Pr)-doped $Pb(Zr, Ti)O_3$ are examples of RFE-I because experiments revealed a clear suppression of the ferroelectricity due to the doping, characterized by the shift of the FE transition point to the low-T side and weakening of the ferroelectricity [23, 24]. The defect model employed here allows us a possibility to investigate the dielectric relaxation behaviours of various types of RFEs into which different kinds of defects or random fields may be doped or imposed.

Unfortunately, up to now we have no direct experimental evidence on the multi-peaked time distribution of the dielectric relaxation. Experimentally, $G(\log\tau, T)$ is derived by equation (9) from experimental χ'–T data at different frequencies. However, due to the limited ω-range covered, the time domain covered by $G(\log\tau, T)$ is limited too. Furthermore, for those RFEs often studied, like $Pb(Mg_{1/3}Nb_{2/3})O_3$, Zr(Hf)-doped $BaTiO_3$ and La(Pr)-doped $Pb(Zr, Ti)O_3$, the diffusive phase transitions occur at relatively high temperature. The thermal flip times for dipoles or dipole clusters between normal FEs and RFEs may not be very different in order of magnitude, which does not allow a reliable checking of the multi-peaked distribution. Nevertheless, it would be possible to check this predicted effect if an RFE with phase transition point as low as 100 K or even lower can be developed, in which the relaxation timescale may be as broad as or more than 10–20 orders of magnitude. For such cases, we expect a multi-peaked time-domain distribution of the dielectric relaxation.

It may be a reasonable argument that due to the intrinsic inhomogeneity of samples for experiments, the evaluated time distribution from the measured dielectric relaxation remains single-peaked. However, it can be expected that in 3D lattices the dimensional correlation among FE nanoclusters could be even more considerable, thus resulting in a multi-peaked distribution of the dielectric relaxation. In fact, with a high enough ac field, the simulated χ'–T and χ''–T curves remain diffusive and single-peaked, although the time-domain distribution is multi-peaked. Figure 5 presents the simulated χ'–T and χ''–T curves for $C_0 = 0.5$ and $C_p = 0.5$ at different ω under $E_m = 15.0$. The distribution $G(\log\tau, T)$ for this system is shown in figure 4 (open circles). All typical features for RFEs as observed commonly are shown in figure 5, including significant frequency dispersion and broad transition regime.

Although a detailed analysis on these simulated features will be presented elsewhere [19], here we present the fitting to the simulated data by the Vogel–Fulcher relationship, a well-believed behaviour for RFEs. This relation reads [4]

$$\omega = \omega_{00} \cdot \exp\left(-\frac{E_a}{(T_m - T_f)}\right) \tag{10}$$

where ω_{00} is the pre-exponential factor, E_a the thermal-activation energy for the dipole clusters, T_m the peak temperature for χ'–T curves and T_f the frozen point below which the clusters are essentially frozen and the thermally driven relaxation becomes negligible.

We evaluate the values of T_m at different ω from figure 5(a) and then plot $\ln(\omega)$ as a function of $1/(T_m - T_f)$ where T_f is treated as a best-fitted parameter. Unfortunately, the best fitting of the data using a linear $\ln(\omega) - 1/(T_m - T_f)$ relation cannot be obtained unless $T_f = 0$ is set. The result is presented in figure 6 by setting $T_f = 0$. In fact, it is shown that even for $T_f = 0$ the data do not yet follow the linear relation in a satisfactory sense, although a roughly linear dependence between $\ln(\omega)$ and $1/T_m$ can be argued. It should be noted that equation (10) recovers the typical Debye thermal-activation behaviour (Arrhenius law) over the whole T-range until $T = 0$ as the low-T limit.

Two possible reasons for this deviation from the Vogel–Fulcher behaviour may be argued. First, the model employed here for describing the defect-induced RFE only takes into account the Debye mechanism. The dielectric susceptibility is calculated based on pure thermally activated relaxation. Because T_f is the temperature below which the dipole relaxation by the

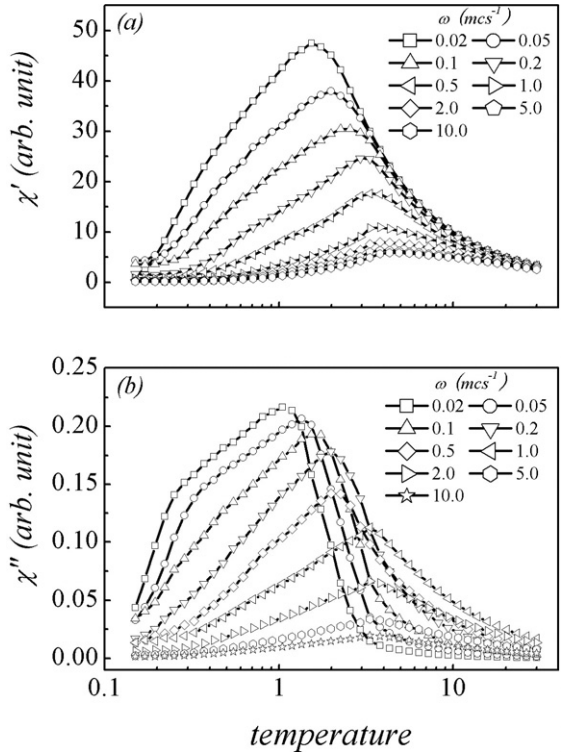

Figure 5. Simulated dielectric susceptibility (real and imaginary parts) as a function of T for different ac field frequencies: (a) χ'–log(T) curves and (b) χ''–log(T) curves. $C_0 = 0.5$, $C_p = 0.5$ and $E_m = 15.0$.

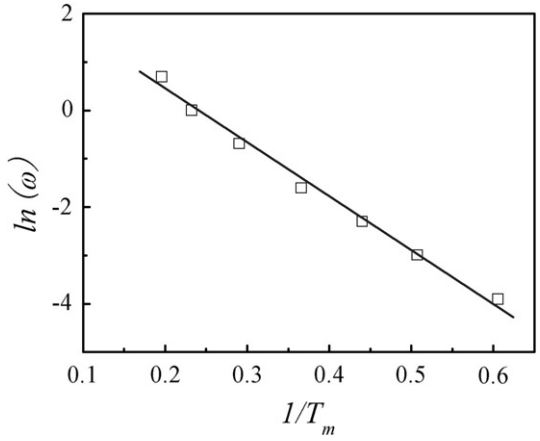

Figure 6. Peak frequency ω of the dielectric susceptibility as a function of temperature T. $C_0 = 0.5$, $C_p = 0.5$ and $E_m = 15.0$. See text.

Debye mechanism can no longer be possible, it is thus natural that the frozen temperature $T_\mathrm{f} \to 0$ is shown in figure 6. Secondly, since the dielectric relaxation itself is polydispersive in timescale, the dielectric susceptibility as a function of T may be viewed as a summation over

the polydispersive time distribution of the relaxation. Therefore, the present simulation over a finite lattice size may not be sufficient to check the Vogel–Fulcher behaviour. An extensive simulation over a much bigger lattice is going on.

It should be pointed out here that the time-domain distribution of the dielectric relaxation depends also on the distribution of the random field. A monotonic or diffusive single-peaked distribution is also possible if parameter b_m takes a Gaussian-like distribution within $[-1, 1]b_M$. Similar works were reported earlier [25], although no time-domain distribution of the dielectric relaxation was given in detail.

4. Conclusion

In conclusion, we have presented a Monte Carlo simulation on the time-domain distribution of dielectric relaxation for an RFE employing the Ginzburg–Landau theory on ferroelectrics. By introducing the dipole defects into the FE lattice we have successfully reproduced the two-phase coexistence of RFEs where FE nanoclusters are embedded in the PE matrix. The evaluated time-domain distribution of the dielectric relaxation below the FE transitions exhibits a multi-peaked pattern with multi-characteristic times instead of a monotonic or diffusive single-peaked pattern, although the dynamic dielectric dispersions remain single-peaked and diffusive. The multi-characteristic times (peaked times) reflect the significance of local dipole–cluster interactions in RFEs. The present work sheds light on our conventional understanding of the relaxation dynamics in RFEs.

Acknowledgments

This work was supported by the Hong Kong Polytechnic University through project I-BBZ3. JML acknowledges the support from the Natural Science Foundation of China (50332020, 10021001, 10494037) and National Key Projects for Basic Researches of China (2004CB619004).

References

[1] Pirc P and Blinc R 1999 *Phys. Rev.* B **60** 13470
[2] Blinc R, Laguta V and Zalar B 2003 *Phys. Rev. Lett.* **91** 247601
[3] Vakhrushev S B and Shapiro S M 2004 *Phys. Rev.* B **70** 134110
[4] Glazounov A E and Tagantsev A K 2000 *Phys. Rev. Lett.* **85** 2192
[5] Viehland D, Jang S J, Cross L E and Wutting M 1990 *J. Appl. Phys.* **68** 2916
Viehland D, Jang S J, Cross L E and Wutting M 1991 *Phys. Rev.* B **43** 8316
[6] Pirc R, Blinc R and Kutnjak Z 2002 *Phys. Rev.* B **65** 214101
[7] Tyunina M and Levoska J 2001 *Phys. Rev.* B **63** 224102
Tyunina M and Levoska J 2005 *Phys. Rev.* B **72** 104112
Tyunina M and Levoska J 2005 *J. Appl. Phys.* **97** 114107
[8] Cross L E 1987 *Ferroelectrics* **76** 241
[9] Vugmeister B E and Glinchuk M D 1990 *Rev. Mod. Phys.* **62** 993
[10] Cheng Z Y, Katiyar R S, Yao X and Bhalla A S 1998 *Phys. Rev.* B **57** 8166
[11] Tagantsev A K 1994 *Phys. Rev. Lett.* **72** 1100
[12] Colla E V, Furman E L, Gupta S M, Yushin N K and Viehland D 1999 *J. Appl. Phys.* **85** 1693
[13] Bobnar V, Kutnjak Z and Levstik A 2000 *Appl. Phys. Lett.* **76** 2773
[14] Kircher O, Schiener B and Böhmer R 1998 *Phys. Rev. Lett.* **81** 4520
Kircher O, Diezemann G and Böhmer R 2001 *Phys. Rev.* B **64** 054103
[15] Yao X, Chen Z and Cross L E 1983 *J. Appl. Phys.* **54** 3399
[16] Semenovskaya S and Khachaturyan A G 1998 *J. Appl. Phys.* **83** 5125
[17] Zhang Q M, Zhao J, Shrout T R and Cross L E 1997 *J. Mater. Res.* **12** 1777
Park C H and Chadi D J 1998 *Phys. Rev.* B **57** 13961

Wu Z, Duan W, Wang Y, Gu B L and Zhang X W 2003 *Phys. Rev.* B **67** 052101
Courtens E 1984 *Phys. Rev. Lett.* **52** 69
Su C C, Vugmeister B and Khachaturyan A G 2001 *J. Appl. Phys.* **90** 6345
[18] Liu J-M, Wang X, Chan H L W and Choy C L 2004 *Phys. Rev.* B **69** 094114
Wang X, Liu J-M, Chan H L W and Choy C L 2004 *J. Appl. Phys.* **95** 4282
[19] Liu J-M, Chan H L W and Choy C L, unpublished
[20] Cao W and Cross L E 1991 *Phys. Rev.* B **44** 5
Nambu S and Sagala D A 1994 *Phys. Rev.* B **50** 5838
Potter B G Jr, Tikare V and Tuttle B A 2000 *J. Appl. Phys.* **87** 4415
[21] Li B L, Liu X P, Fang F, Zhu J L and Liu J-M 2006 *Phys. Rev.* B **73** 014107
[22] Hu H L and Chen L Q 1997 *Mater. Sci. Eng.* A **238** 182
[23] Anwar S, Sagdeo P R and Lalla N P 2006 *Solid State Commun.* **138** 331
[24] Lu Z G and Calvarin G 1995 *Phys. Rev.* B **51** 2694
Zhi Y, Chen A, Guo R and Bhalla A S 2002 *J. Appl. Phys.* **92** 2655
[25] Liu Z R, Gu B L and Zhang X W 2000 *Phys. Rev.* B **62** 1